

# Accretion-powered millisecond pulsars

Juri Poutanen

*Astronomy Division, P.O.Box 3000, FIN-90014, University of Oulu, Finland*

Received 3 October 2005; received in revised form 17 April 2006; accepted 17 April 2006

## Abstract

I review X-ray observations of accretion-powered millisecond pulsars and current theories for formation of their spectra and pulse profiles.

© 2006 COSPAR. Published by Elsevier Ltd. All rights reserved.

*Keywords:* Accretion; Accretion discs; Stars, Neutron; X-rays, Binaries

## 1. Introduction

A number of rapidly spinning neutron stars in low-mass X-ray binaries were discovered with the *Rossi X-ray Timing Explorer (RXTE)* in the recent years. These discoveries confirm the ideas on the formation of radio (recycled) millisecond pulsars in low-mass X-ray binaries (see review by [Bhattacharya, 1995](#)). Accretion of matter onto a neutron star results in an increase in its spin rate to millisecond periods, if the magnetic field of the star is below about  $10^9$  G.

Thirteen sources show nearly coherent oscillations for a few seconds during X-ray bursts at frequencies ranging from 270 to 619 Hz (see [Strohmayer and Bildsten, 2006](#) for a review). These are now called nuclear-powered millisecond pulsars. The number of accretion-powered millisecond pulsar (AMSP) showing pulsations in the persistent emission reached seven by June 2005. A more observationally inclined review of AMSP is given by [Wijnands \(2005\)](#). Here, I concentrate on the results of the X-ray spectroscopy, analysis of pulse profiles, and our present theoretical understanding.

## 2. Pulsars parameters

The first real AMSP SAX J1808.4–3658 was discovered in 1998 by [Wijnands and van der Klis \(1998\)](#). Now

(September 2005) there are seven AMSPs with spin frequencies from 185 up to 599 Hz (see [Table 1](#)). The fastest AMSP, IGR J00291 + 5934 with the period of just 1.67 ms is the fifth fastest among all known pulsars (including radio- and nuclear-powered MSPs). The last AMSP HETE J1900.1–2455 was discovered in June 2005.

AMSPs show pulse frequency variations. These observations are very important for understanding of the evolution of the neutron stars in low-mass X-ray binaries towards radio MSPs. They would also shed some light on a complicated problem of the interaction of the magnetosphere with the accretion flow. One expects a spin-up rate

$$\dot{\nu} = 3.7 \times 10^{-13}$$

$$\times \frac{L_{37}}{\eta_{-1} I_{45}} \left( \frac{R_m}{R_{co}} \right)^{1/2} \left( \frac{M}{1.4 M_\odot} \right)^{2/3} \left( \frac{v_{spin}}{600} \right)^{-1/3} \text{ Hz s}^{-1},$$

where (notation  $Q = 10^x Q_x$  in cgs units is used)  $I$  is the neutron star moment of inertia,  $L$  is the luminosity,  $\eta$  is the accretion efficiency,  $R_m$  and  $R_{co}$  are the magnetospheric and corotation radii. Some reported  $\dot{\nu}$  are, however, *negative* implying pulsar slowing down during the outburst ([Galloway et al., 2002](#); [Morgan et al., 2003](#)). [Markwardt \(2004\)](#) finds wild swings in the apparent spin frequency of both signs resulting in the total fractional phase shift less than 0.15. These could be, however, artifacts of the pulse profile variations (see Section 4). The reported positive  $\dot{\nu} \sim 8 \times 10^{-13}$  Hz/s for IGR J00291 + 5934 ([Falanga et al., 2005b](#)) is larger than expected by a factor of 5 (since

*E-mail address:* [jpoutane@sun3.oulu.fi](mailto:jpoutane@sun3.oulu.fi)

Table 1  
Parameters of the accretion-powered millisecond pulsars

	Source	$P_{\text{orb}}^{\text{a}}$ (min)	$\nu_{\text{spin}}^{\text{b}}$ (Hz)	$a_x \sin i^{\text{c}}$ (lt-ms)	$f_x^{\text{d}}$ ( $M_{\odot}$ )	$M_{\text{c,min}}^{\text{e}}$ ( $M_{\odot}$ )
1	SAX J1808.4–3658	121	401	62.809	$3.779 \times 10^{-5}$	0.043
2	XTE J1751–305	42.4	435	10.113	$1.278 \times 10^{-6}$	0.014
3	XTE J0929–314	43.6	185	6.290	$2.9 \times 10^{-7}$	0.0083
4	XTE J1807–294	40.1	191	4.75	$1.49 \times 10^{-7}$	0.0066
5	XTE J1814–338	257	314	390.3	$2.016 \times 10^{-3}$	0.17
6	IGR J00291+5934	147	599	64.993	$2.813 \times 10^{-5}$	0.039
7	HETE J1900.1–2455	83.3	377	18.39	$2.00 \times 10^{-6}$	0.016

References: [1] Wijnands and van der Klis (1998); Chakrabarty and Morgan (1998); [2] Markwardt and Swank (2002); Markwardt et al. (2002); [3] Remillard et al. (2002); Galloway et al. (2002); [4] Markwardt et al. (2003a); Kirsch et al. (2004); Falanga et al. (2005a); [5] Markwardt and Swank (2003); Markwardt et al. (2003b); [6] Eckert et al. (2004); Markwardt et al. (2004a,b); Galloway et al. (2005); [7] Vanderspek et al. (2005); Morgan et al. (2005); Kaaret et al. (2005).

<sup>a</sup> Orbital period.

<sup>b</sup> Neutron star spin frequency.

<sup>c</sup> Projected semimajor axis.

<sup>d</sup> Pulsar mass function.

<sup>e</sup> Minimum companion mass for a  $M_x = 1.4 M_{\odot}$  neutron star.

$L_{37} \sim 0.37$ ). A positional error of  $\sim 0''.7$  could result in such a large derivative, while the radio position is known with a  $0''.1$  accuracy (Rupen et al., 2004). The motion of the radio source itself does not produce an error larger than  $\sim 0''.3$  (for the distance of 5 kpc) a week after the outburst, confirming the reality of the pulsar spin-up and possibly implying a small moment of inertia  $I$ .

Accretion-powered pulsars reside in very compact binary systems with orbital periods ranging from 40 min to 4.3 h. Surprisingly three out of 7 pulsars have  $42 \pm 2$  min orbits. Adding to this set also 4U1626-67, 4U1916-05, and X1832-330 (in globular cluster NGC 6652) with orbital periods of 42, 50, and 44 min, respectively, it becomes clear that this interesting fact deserves some explanation (see Nelson and Rappaport, 2003, for a possible scenario). The pulsar mass function

$$f_x = (M_c \sin i)^3 / (M_c + M_x)^2 = 4\pi^2 (a_x \sin i)^3 / GP_{\text{orb}}^2$$

is very low for all these objects, implying extremely low companion masses consistent with degenerate white (helium or carbon–oxygen) or brown dwarfs (Bildsten and Chakrabarty, 2001; Markwardt et al., 2002; Galloway et al., 2002; Falanga et al., 2005a; Galloway et al., 2005) except XTE J1814–338 which contains probably a hydrogen-rich star (Krauss et al., 2005). All AMSPs are transients with the outbursts repeating every few years and lasting a few weeks. They have a rather low time-average accretion rate of  $\sim 10^{-11} M_{\odot}/\text{yr}$ , which could be the main reason why the magnetic field is still strong enough for pulsations to be observed (Cumming et al., 2001).

### 3. Broad-band X-ray spectra

The broad-band coverage of the *RXTE* together with *XMM* gave a possibility for studying the spectra of AMSP in great detail. The spectra can be modelled by three

components: two soft, thermal looking ones below a few keV and a power-law like tail (see Fig. 1).

The two soft components which can be modelled as thermal emission from a colder ( $kT \sim 0.4$ – $0.6$  keV) accretion disc and a hotter ( $\sim 1$  keV) spot on the neutron star surface. The softer components in XTE J1751–305 and XTE J1807–294 are studied with *XMM* by Gierliński and Poutanen (2005); Falanga et al. (2005a). The inferred inner disk radius  $R_{\text{in}} \sim (10$ – $15)\text{km}/\sqrt{\cos i}$  is consistent with the flow disrupted by the neutron star magnetosphere within a couple of stellar radii. The hotter black body normalization corresponding to the area of  $\sim 30$ – $100 \text{ km}^2$  and its pulsation are consistent with it being produced in a spot at the neutron star surface.

A power-law tail (having spectral photon index  $\Gamma \sim 1.8$ – $2.1$ ) shows a cutoff around 100 keV and can be fitted with thermal Comptonization. The electron temperature of the Comptonizing medium is around  $kT_e \sim 20$ – $60$  keV and Thomson optical depth of  $\tau_T \sim 0.7$ – $2.5$  (for a plane-parallel slab geometry) (Gierliński et al., 2002; Poutanen and Gierliński, 2003; Gierliński and Poutanen, 2005; Falanga et al., 2005a). Weakness of the Compton reflection from the disk indicates that the solid angle covered by the disk as viewed from the main emission source (accretion shock) is small, being consistent with  $R_{\text{in}} \sim 40 \text{ km}$  (Gierliński and Poutanen, 2005).

The broad-band X-ray spectra of AMSPs are very similar to each other. They also show very little variability during the outbursts (see e.g., Gilfanov et al., 1998; Gierliński and Poutanen, 2005; Falanga et al., 2005b). When fitting spectra with thermal Comptonization models, one also finds that the product of the electron temperature and optical depth is almost invariant (e.g.  $[kT_e, \tau_T] = [60 \text{ keV}, 0.88]$  in SAX J1808.4–3658;  $[33 \text{ keV}, 1.7]$  in XTE J1751–305,  $[37 \text{ keV}, 1.7]$  in XTE J1807–294,  $[49 \text{ keV}, 1.12]$  in IGR J00291+5934; see Gierliński and Poutanen, 2005; Falanga et al., 2005a,b). The constancy of the spectral slope can be

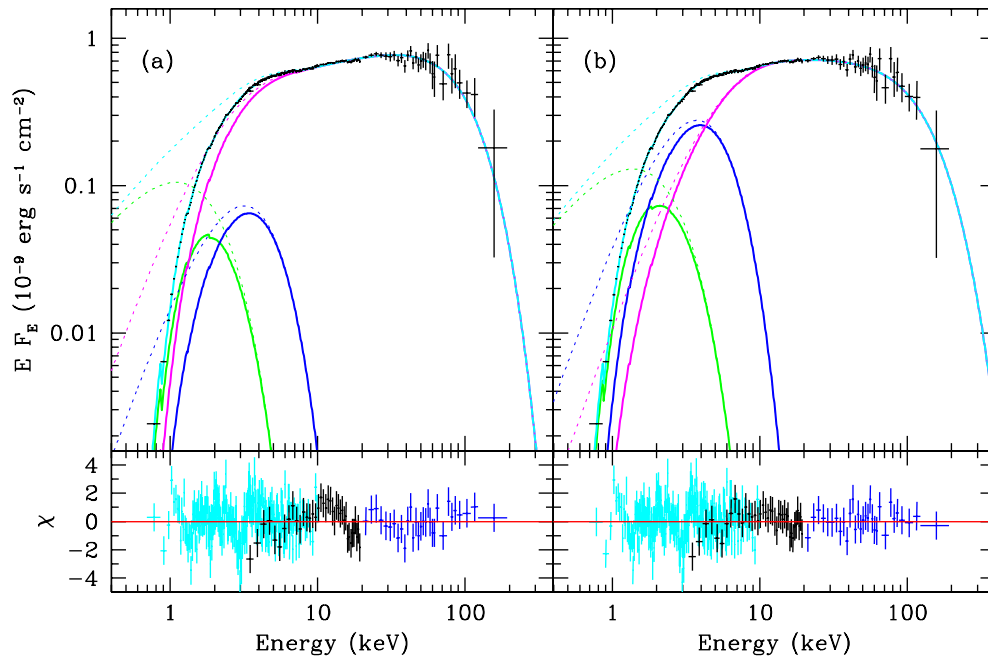


Fig. 1. Spectrum of XTE J1751–305 as observed by *XMM*/EPIC-pn, *RXTE*/PCA and HEXTE. The models consists of the multicolour disc (peaking at  $\sim 1$  keV), single-temperature blackbody (peaking at 3–4 keV), and thermal Comptonization of the blackbody photons. The dotted curves show unabsorbed spectral components. Panel (a) shows a model where seed photons for Comptonization have the same temperature as the blackbody photons, while in panel (b) the seed photons are hotter. The lower panels shows the residuals. See Gierliński and Poutanen (2005) for details.

used as an argument that the emission region geometry does not vary much with the accretion rate. If the energy dissipation takes place in a hot shock, while the cooling of the electrons is determined by the reprocessing of the hard X-ray radiation at the neutron star surface (two-phase model, e.g. Haardt and Maraschi, 1993; Poutanen and Svensson, 1996; Malzac et al., 2001), the spectral slope is determined by the energy balance in the hot phase and, therefore, by the geometry.

#### 4. Phase-resolved spectroscopy, pulse profiles, and time lags

The pulse profiles from AMSPs are rather close to sinusoidal with peak-to-peak oscillation amplitude  $A = (F_{\max} - F_{\min}) / (F_{\max} + F_{\min})$  between 4 (in XTE J1751–305) and 12 per cent (in XTE J1814–338). At energies above 50 keV the *INTEGRAL* data on IGR J00291+5934 show the increase of the pulse amplitude up to  $\sim 25$  per cent (Falanga et al., 2005b). Deviations from the sine wave are stronger at higher energies (see Fig. 2). The harmonic content also is stronger when  $A$  is larger (e.g. the harmonic-to-fundamental ratio is  $\sim 0.03$  in XTE J1751–305 (Gierliński and Poutanen, 2005), while it is  $\sim 0.33$  in XTE J1814–338 (Strohmayer et al., 2003).

Pulse profiles at higher energies reach their peaks at an earlier phase relative to the soft photons resulting in the soft time lags. In SAX J1808.4–3658 (Cui et al., 1998; Gierliński et al., 2002), XTE J1751–305 (Gierliński and Poutanen, 2005), and XTE J0929–314 (Galloway et al., 2002) the lags increase (in absolute value) with energy up to about 7–10 keV after they saturate (see Fig. 3, left

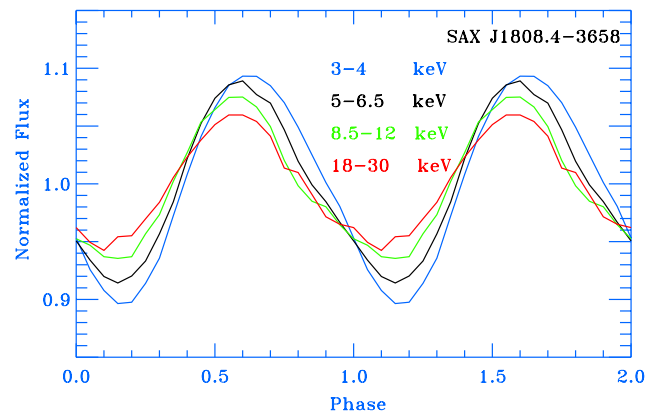


Fig. 2. Normalized pulse profiles of SAX J1808.4–3658 at different energies during the April 1998 outburst.

panel). In IGR J00291+5934 (see Fig. 3, right panel; Galloway et al., 2005; Falanga et al., 2005b), the behaviour is more complicated and the lags decrease between 7 and 15 keV, seemingly saturating at higher energies.

One can point out that the contribution of the black body decreases exponentially with energy and the lags increase significantly at the same time. Above  $\sim 7$  keV, the blackbody's contribution is negligible and the lags saturate. When fitting phase-resolved spectra with a two-component model (blackbody + Comptonization), one clearly sees that the normalizations of the components do not vary in phase, with black body lagging the Comptonized emission (see Fig. 4 and Gierliński et al., 2002; Gierliński and Poutanen, 2005). In SAX J1808.4–3658 the profile

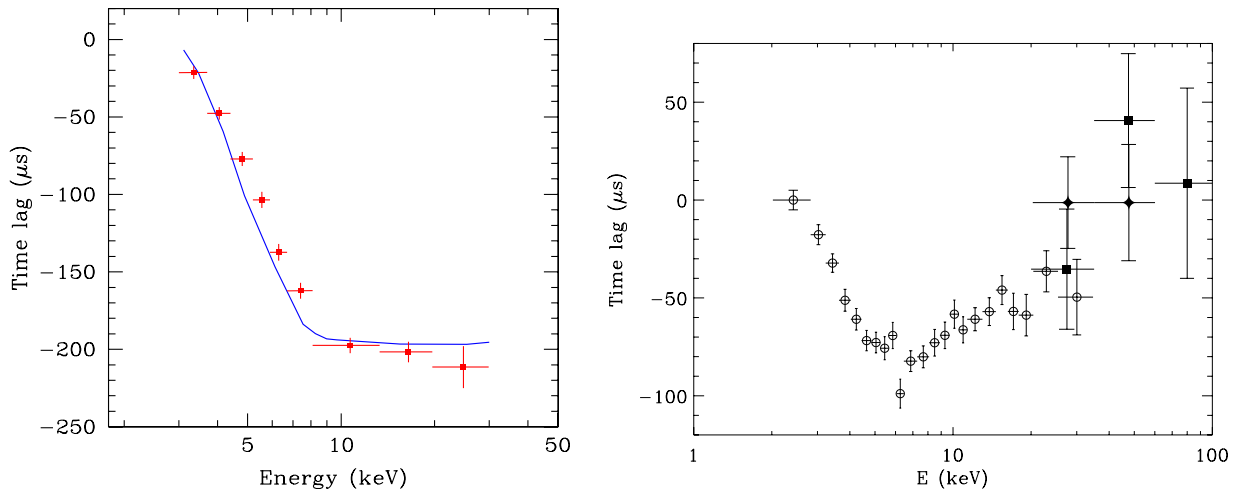


Fig. 3. Time lags as a function of energy for SAX J1808.4–3658 (left panel; Gierliński et al., 2002) and IGR J00291+5934 (right panel; Falanga et al., 2005b).

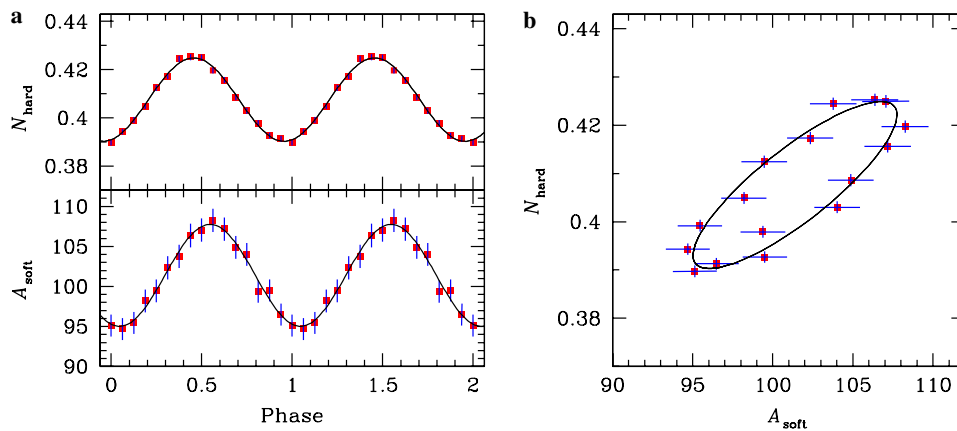


Fig. 4. Pulsation of the two model components, blackbody and Comptonization, in XTE J1751–305. From Gierliński and Poutanen (2005).

corresponding to the Comptonized emission is clearly non-sinusoidal. Difference in profiles of the two components can be explained by their different emission pattern (Poutanen and Gierliński, 2003). Its variation may cause pulse shape change resulting in the swings of  $\dot{\nu}$  discussed in Section 2.

## 5. Modelling the pulse profiles of AMSPs

It is generally believed that the bulk of the X-ray emission observed from AMSPs originates from polar caps where the gas stream channels by the neutron star magnetic field impacts the stellar surface, forming a shock. This is supported by a weak energy dependence of the variability amplitude and a fairly constant spectral shape as a function of pulse phase (any additional source of radiation would have to have a spectrum identical to that of the shock), as well as the observed broadening of the pulse peak in the power-spectrum of SAX J1808.4–3658 due to modulation of the aperiodic variability by the spin period (Menna et al., 2003).

### 5.1. Computing pulse profiles

Pulse profile shape and variability amplitude carry the information about the compactness of the neutron star, spot size and its position at the star, and the emission pattern. Gravitational light bending tends to decrease the pulse amplitude (Pechenick et al., 1983; Riffert and Mészáros, 1988; Page, 1995; Leahy and Li, 1995; Beloborodov, 2002). An earlier attempt to incorporate the effect of rapid rotation using Kerr metric (Chen and Shaham, 1989) did not include the dominant Doppler boost caused by the star's surface motion in the locally non-rotating frame. This was criticized by Braje et al. (2000). They also noticed that Doppler boost and light travel time delays are important for shaping the profiles, while the frame dragging affects them at a  $\sim 1\%$  level. The Monte-Carlo simulations used by Braje et al. (2000) for the light curve calculation are, however, extremely time-consuming and are hardly suitable for data fitting.

As frame dragging is not so important, one can consider Schwarzschild metric instead. One can account for Doppler

effect making Lorentz transformation from the frame rotating with the star to a non-rotating frame and then follow light trajectory in the Schwarzschild space-time to infinity (“Schwarzschild + Doppler” or SD approach). An attempt to formulate the problem was done by Miller and Lamb (1998) who considered the spot and the observer in the equatorial plane only. Oscillation waveforms and amplitudes for arbitrary spot and observer position were computed by Weinberg et al. (2001) and Munro et al. (2002). However, these papers provided no details on how to account for effect of aberration on intensity and projected spot area. A formalism for computing the pulse profiles accounting for Doppler boosting, relativistic aberration and gravitational bending was given in Poutanen and Gierliński (2003). Effects of the anisotropy of Comptonized radiation from a shock on the light curves and polarization were studied by Viironen and Poutanen (2004). Analytical formulae for oscillation amplitudes are presented by Poutanen (2004). Light curves from realistic spots produced by accretion onto inclined magnetic dipole are computed by Kulkarni and Romanova (2005) using formalism of Poutanen and Gierliński (2003); Viironen and Poutanen (2004); Beloborodov (2002). Accuracy of the SD approach is discussed by Cadeau et al. (2005).

### 5.2. Main effects

Let us now briefly describe the main effects shaping the pulse profiles of AMSPs. Without general or special relativistic effects, a small black body spot would produce sinusoidal variations (with possible eclipses) due to a change of the projected area. Light bending reduces the variability amplitude (compare dotted and dashed curves in Fig. 5), while

the pulse remains almost sinusoidal (Beloborodov, 2002). Relativistic aberration and Doppler boosting modify the observed flux for a rapidly spinning star. The projected area is changed by the Doppler factor  $\delta$  due to aberration, and the frequency-integrated specific intensity is multiplied by  $\delta^4$  (see Poutanen and Gierliński, 2003). Since  $\delta$  reaches the maximum a quarter of the period earlier than the projected area (Fig. 5b), the pulse becomes skewed to the left (see Fig. 5 and compare it to Fig. 2). Light travel time delays slightly modify the profile further (note that time delays are already accounted for in the flux calculations by one of the Doppler factors).

### 5.3. Oscillation amplitudes

Due to the combined action of the Doppler effect and time delays, the pulse profile deviates from a simple sine wave. (We consider below the situation where the spot is always visible.) The relative amplitudes (in the bolometric signal) of the harmonic  $A_1$  to that of the fundamental  $A_0$  grows approximately linearly with the rotational frequency (Poutanen, 2004):

$$\frac{A_1}{A_0} \approx \frac{5}{2} \frac{2\pi R}{c} v_{\text{spin}} \sin i \sin \theta = 0.16 \frac{R}{10 \text{ km}} \frac{v_{\text{spin}}}{300 \text{ Hz}} \sin i \sin \theta,$$

where  $i$  is the inclination and  $\theta$  is the polar angle of the spot center. Even a slight deviation from the isotropic emission (e.g. in the form  $I(\alpha) \propto 1 + b \cos \alpha$ , where  $\alpha$  is the angle from the spot normal and  $b$  is the anisotropy parameter) leads to a high harmonic content (Poutanen and Gierliński, 2003; Poutanen, 2004; Viironen and Poutanen, 2004):

$$\frac{A_1}{A_0} = \frac{b(1 - R_s/R)/2 \sin i \sin \theta}{1 + 2b[R_s/R + (1 - R_s/R) \cos i \cos \theta]},$$

where  $R_s = 2GM/c^2$ . The harmonic content  $A_1/A_0$  as well as the total rms are proportional to  $\sin i \sin \theta$  (Beloborodov, 2002; Poutanen and Gierliński, 2003, 2004; Poutanen, 2004). Therefore, one expects harmonics to be relatively strong when the rms is larger, which is exactly what is observed. Increasing the spot size leads to a reduction of the amplitude of the harmonic first and of the total rms later (Weinberg et al., 2001; Poutanen, 2004).

If the spectrum has a sharp cutoff, the rms amplitude of the pulse at energies above the cutoff increases dramatically. The flux varies as  $\propto \delta^{3+\Gamma}$  (Poutanen and Gierliński, 2003; Viironen and Poutanen, 2004), where  $\Gamma(E) = 1 - d \ln F_E / d \ln E$  is the energy-dependent photon spectral index, resulting in the rms energy dependence  $\propto 3 + \Gamma(E)$ . For the spectrum in the form  $F_E \propto E^{-(\Gamma_0-1)} \exp(-[E/E_c]^\beta)$ , which is typical for Comptonization, the photon index  $\Gamma(E) = \Gamma_0 + \beta(E/E_c)^\beta$ . At low energies,  $\Gamma \approx \Gamma_0$ , and rms is a very weak function of energy. Close to the cutoff, the spectral index rapidly increases, resulting in a significant growth of the rms, as observed in the *INTEGRAL* data for IGR J00291+5934 (Falanga et al., 2005b). In case of coherent oscillations observed during X-ray bursts, a linear increase

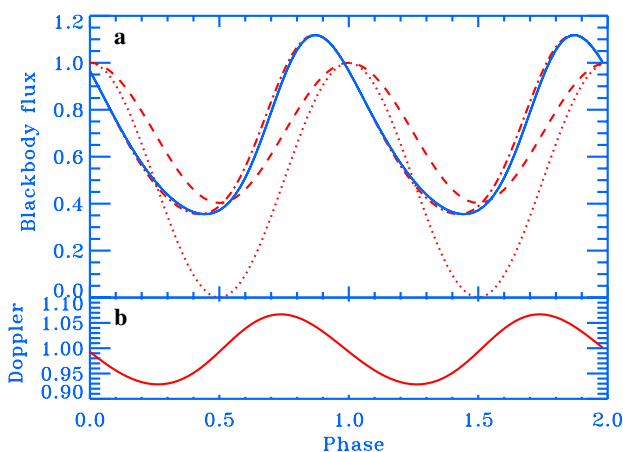


Fig. 5. Pulse profile for a small black body spot at the neutron star surface. (a) Dotted curve shows the profile for a slowly rotating star in Newtonian approximation. Gravitational light bending reduces variability amplitude (dashed curve). Doppler effect due to rapid rotation skews the profile (dot-dashed curves). Accounting for the light travel delays further modifies the profile slightly (solid curve). (b) Doppler factor as a function of phase. We assumed neutron star mass  $M = 1.4 M_\odot$  and radius  $R = 10.3 \text{ km}$ , rotational frequency  $\nu = 600 \text{ Hz}$ , the inclination  $i = 45^\circ$ , and the polar angle of the spot center  $\theta = 45^\circ$ .



of the rms with energy is expected, since the spectrum is close to a blackbody which has an exponential cutoff (see also Miller and Lamb, 1998; Munro et al., 2003).

#### 5.4. Constraints on the neutron star equation of state and spot parameters

The amplitude of variability and the pulse shape (harmonic content) can be used to put constraints on the compactness of the neutron star, position, size and the emission pattern of a radiating spot. In case of the coherent oscillations observed during the X-ray bursts the constraints on the compactness are not very tight (Miller and Lamb, 1998; Nath et al., 2002; Bhattacharyya et al., 2005). A very weak harmonic content led to the conclusion that the bright region (or the line of sight) must be near the rotational pole or must cover half of the star (Munro et al., 2002). Fitting the pulse profile shape (but not the amplitude) of the oscillations observed during the X-ray burst of XTE J1814–338 was performed by Bhattacharyya et al. (2005), with a resultant preferred spot polar angle  $\theta = 90^\circ \pm 30^\circ$ . This appears improbable, since an identical (in shape and phase) pulse observed in the persistent emission (Strohmayer et al., 2003) would require the magnetic poles to lie at the equator, in which case the antipodal spot should also be visible.

For AMSPs the statistics in the pulse profiles is much better since the pulse is folded over a longer observational period (days or weeks rather than seconds as in the case of X-ray bursts). This allows one to obtain tight constraints on the neutron star compactness in SAX J1808.4–3658 as well as the emission pattern (consistent with Comptonization from the plane-parallel shock), inclination, and the spot polar angle (see Poutanen and Gierliński, 2003, and Fig. 6).

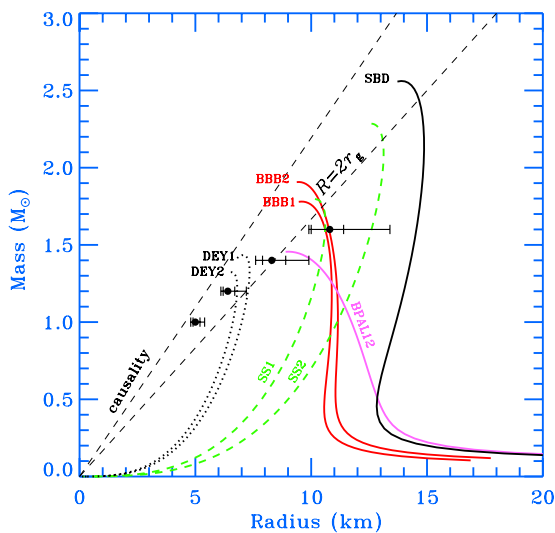


Fig. 6. Constraints on the neutron star mass-radius relation obtained by fitting the pulse profiles of SAX J1808.4–3658 (filled circles with error bars) together with a set of equations of state for neutron and strange stars. From Poutanen and Gierliński (2003).

## 6. Summary

We have reviewed here X-ray observations of the AMSPs, concentrating on the broad-band spectra and the energy-dependent pulse profiles. Recent advances in the theoretical modelling of the spectral and timing characteristics are also described. At the observational side, we are missing the details of the pulse profile and spectral evolution during the outbursts. One would expect that a changing accretion rate would force a change in the accretion pattern on to a neutron star surface, causing corresponding profile variations. Detailed studies of the reflection amplitude and frequencies of quasi-periodic oscillations should reveal changes in the inner disk radius during outbursts. The pulse profile should also react correspondingly as the visibility of the antipodal spot depends on the disk radius. Combined with the spin-up rate observations, these would shed some light on a complicated problem of the magnetosphere interaction with the accretion flow. On the theoretical side, we need a detailed model describing the dynamics of the accretion flow onto the neutron star surface including radiation feedback. It is not clear yet what fraction of the material follows the magnetic field lines towards the poles. The impact of the realistic spot geometry and the radiation pattern on the pulse profiles and the derived parameters should be studied further.

## Acknowledgements

This work is supported by the Academy of Finland, the Jenny and Antti Wihuri Foundation, the Vilho, Yrjö and Kalle Väisälä Foundation.

## References

- Beloborodov, A.M. Gravitational bending of light near compact objects. *ApJ* 566, L85–L88, 2002.
- Bhattacharyya, D. Millisecond pulsars, in: Lewin, W.H.G., van Paradijs, J., van den Heuvel, E.P.J. (Eds.), *X-ray Binaries*. Cambridge University Press, Cambridge, pp. 233–251, 1995.
- Bhattacharyya, S., Strohmayer, T.E., Miller, M.C., Markwardt, C.B. Constraints on neutron star parameters from burst oscillation light curves of the accreting millisecond pulsar XTE J1814–338. *ApJ* 619, 483–491, 2005.
- Bildsten, L., Chakrabarty, D. A brown dwarf companion for the accreting millisecond pulsar SAX J1808.4–3658. *ApJ* 557, 292–296, 2001.
- Braje, T.M., Romani, R.W., Rauch, K.P. Light curves of rapidly rotating neutron stars. *ApJ* 531, 447–452, 2000.
- Cadeau, C., Leahy, D.A., Morsink, S.M. Pulse shapes from rapidly rotating neutron stars: equatorial photon orbits. *ApJ* 618, 451–461, 2005.
- Chakrabarty, D., Morgan, E.H. The two-hour orbit of a binary millisecond X-ray pulsar. *Nature* 394, 346–348, 1998.
- Chen, K., Shaham, J. Pulse sharpness and asymmetry in millisecond pulsars. *ApJ* 339, 279–290, 1989.
- Cui, W., Morgan, E.H., Titarchuk, L.G. Soft phase lags in the millisecond X-ray pulsar SAX J1808.4–3658. *ApJ* 504, L27–L30, 1998.
- Cumming, A., Zweibel, E., Bildsten, L. Magnetic screening in accreting neutron stars. *ApJ* 557, 958–966, 2001.
- Eckert, D., Walter, R., Kretschmar, P., et al. IGR J00291+5934, a new X-ray transient discovered with INTEGRAL. *ATel*, 352, 2004.

- Falanga, M., Bonnet-Bidaud, J.M., Poutanen, J., et al. INTEGRAL/RXTE/ XMM-Newton observations of the accreting millisecond pulsar XTE J1807–294 in outburst. *A&A* 436, 647–652, 2005a.
- Falanga, M., Kuiper, L., Poutanen, J., et al. INTEGRAL and RXTE observations of accreting millisecond pulsar IGR J00291+5934 in outburst. *A&A* 444, 15–24, 2005b.
- Galloway, D.K., Chakrabarty, D., Morgan, E.H., Remillard, R.A. Discovery of a high-latitude accreting millisecond pulsar in an ultracompact binary. *ApJ* 576, L137–L140, 2002.
- Galloway, D.K., Markwardt, C.B., Morgan, E.H., et al. Discovery of the accretion-powered millisecond X-ray pulsar IGR J00291+5934. *ApJ* 622, L45–L48, 2005.
- Gierliński, M., Poutanen, J. Physics of accretion in the millisecond pulsar XTE J1751–305. *MNRAS* 359, 1261–1276, 2005.
- Gierliński, M., Done, C., Barret, D. Phase-resolved X-ray spectroscopy of the millisecond pulsar SAX J1808.4–3658. *MNRAS* 331, 141–153, 2002.
- Gilfanov, M., Revnivtsev, M., Sunyaev, R., Churazov, E. The millisecond X-ray pulsar/burster SAX J1808.4–3658: the outburst light curve and the power law spectrum. *A&A* 338, L83–L86, 1998.
- Haardt, F., Maraschi, L. X-ray spectra from two-phase accretion disks. *ApJ* 413, 507–517, 1993.
- Kaaret, P., Morgan, E., Vanderspek, R. Orbital parameters of HETE J1900.1–2455. *ATel*, 538, 2005.
- Kirsch, M.G.F., Mukerjee, K., Breittellner, M.G., et al. Studies of orbital parameters and pulse profile of the accreting millisecond pulsar XTE J1807–294. *A&A* 423, L9–L12, 2004.
- Krauss, M.I., Wang, Z., Dullighan, A., et al. The X-ray position and optical counterpart of the accretion-powered millisecond pulsar XTE J1814–338. *ApJ* 627, 910–914, 2005.
- Kulkarni, A.K., Romanova, M.M. Variability profiles of millisecond X-ray pulsars: results of pseudo-newtonian three-dimensional magnetohydrodynamic simulations. *ApJ* 633, 349–357, 2005.
- Leahy, D.A., Li, L. Including the effect of gravitational light bending in X-ray profile modelling. *MNRAS* 277, 1177–1184, 1995.
- Malzac, J., Beloborodov, A.M., Poutanen, J. X-ray spectra of accretion discs with dynamic coronae. *MNRAS* 326, 417–427, 2001.
- Markwardt, C.B. Millisecond pulsations from LMXBs: future observational considerations, in: Kaaret, P., Lamb, F.K., Swank, J.H. (Eds.), *X-ray Timing 2003: Rossi and Beyond*. AIP, Melville, NY, pp. 217–223, 2004.
- Markwardt, C. B., Swank, J. H. XTE J1751–305. *IAUC* 7867 (1), 2002.
- Markwardt, C. B., Swank, J. H. XTE J1814–338. *IAUC* 8144 (1), 2003.
- Markwardt, C. B., Smith, E., Swank, J. H. XTE J1807–294. *IAUC* 8080 (2), 2003a.
- Markwardt, C.B., Swank, J.H., Strohmayer, T.E. Revised orbit and burst oscillations from the millisecond pulsar XTE J1814–33. *ATel*, 164, 2003b.
- Markwardt, C.B., Swank, J.H., Strohmayer, T.E., et al. Discovery of a second millisecond accreting pulsar: XTE J1751–305. *ApJ* 575, L21–L24 (M02), 2002.
- Markwardt, C.B., Swank, J.H., Strohmayer, T.E. IGR J00291+5934 is a 598 Hz X-ray pulsar. *ATel*, 353, 2004a.
- Markwardt, C.B., Galloway, D.K., Chakrabarty, D., et al. Orbit solution for the millisecond pulsar IGR J00291+5934. *ATel*, 360, 2004b.
- Menna, M.T., Burderi, L., Stella, L., et al. Coupling between periodic and aperiodic variability in SAX J1808.4–3658. *ApJ* 589, 503–508, 2003.
- Miller, M.C., Lamb, F.K. Bounds on the compactness of neutron stars from brightness oscillations during X-ray bursts. *ApJ* 499, L37–L40, 1998.
- Morgan E. H., Chakrabarty D., Wijnands R., et al. Spin frequency evolution of the accreting millisecond pulsar SAX J1808.4–3658. American Astronomical Society, HEAD Meeting #7, Abstract #17.29, 2003.
- Morgan, E., Kaaret, P., Vanderspek, R. HETE J1900.1–2455 is a millisecond pulsar. *ATel*, 523, 2005.
- Muno, M.P., Özel, F., Chakrabarty, D. The amplitude evolution and harmonic content of millisecond oscillations in thermonuclear X-ray bursts. *ApJ* 581, 550–561, 2002.
- Muno, M.P., Özel, F., Chakrabarty, D. The energy dependence of millisecond oscillations in thermonuclear X-ray bursts. *ApJ* 595, 1066–1076, 2003.
- Nath, N.R., Strohmayer, T.E., Swank, J.H. Bounds on compactness for low-mass X-ray binary neutron stars from X-ray burst oscillations. *ApJ* 564, 353–360, 2002.
- Nelson, L.A., Rappaport, S. Theoretical considerations on the properties of accreting millisecond pulsars. *ApJ* 598, 431–445, 2003.
- Page, D. Surface temperature of a magnetized neutron star and interpretation of the ROSAT data. 1: dipole fields. *ApJ* 442, 273–285, 1995.
- Pechenick, K.R., Ftaclas, C., Cohen, J.M. Hot spots on neutron stars—the near-field gravitational lens. *ApJ* 274, 846–857, 1983.
- Poutanen, J. The physics of X-ray emission from accreting millisecond pulsars, in: Kaaret, P., Lamb, F.K., Swank, J.H. (Eds.), *X-ray Timing 2003: Rossi and Beyond*. AIP, Melville, NY, pp. 228–231, 2004. Available from: (astro-ph/0401209).
- Poutanen, J., Gierliński, M. On the nature of the X-ray emission from the accreting millisecond pulsar SAX J1808.4–3658. *MNRAS* 343, 1301–1311, 2003.
- Poutanen, J., Gierliński, M. Modelling the pulse profiles of accreting millisecond pulsars and X-ray bursters. *Nucl. Phys. B (Proc. Suppl.)* 132, 640–643, 2004.
- Poutanen, J., Svensson, R. The two-phase pair corona model for active galactic nuclei and X-ray binaries: how to obtain exact solutions. *ApJ* 470, 249–268, 1996.
- Remillard, R. A., Swank, J. H., Strohmayer, T. E. XTE J0929–314. *IAUC* 7893 (1), 2002.
- Riffert, H., Mészáros, P. Gravitational light bending near neutron stars. I—emission from columns and hot spots. *ApJ* 325, 207–217, 1988.
- Rupen, M.P., Dhawan, V., Mioduszewski, A.J. Further radio observations of IGR J00291+5934. *ATel*, 364, 2004.
- Strohmayer, T., Bildsten, L. New views of thermonuclear bursts, in: Lewin, W. H. G, van der Klis, M. (Eds.), *Compact Stellar X-Ray Sources*. Cambridge University Press, Cambridge, in press, 2006. Available from: (astro-ph/0301544).
- Strohmayer, T.E., Markwardt, C.B., Swank, J.H., in 't Zand, J. X-ray bursts from the accreting millisecond pulsar XTE J1814–338. *ApJ* 596, L67–L70, 2003.
- Vanderspek, R., Morgan, E., Crew, G., et al. Possible new X-ray burst source detected by HETE. *ATel*, 516, 2005.
- Weinberg, N., Miller, M.C., Lamb, D.Q. Oscillation waveforms and amplitudes from hot spots on neutron stars. *ApJ* 546, 1098–1106, 2001.
- Viironen, K., Poutanen, J. Light curves and polarization of accretion- and nuclear-powered millisecond pulsars. *A&A* 426, 985–997, 2004.
- Wijnands, R. Accretion-driven millisecond X-ray pulsars, in: *Pulsars New Research*. Nova Science Publishers, New York, in press, 2005. Available from: [astro-ph/0501264].
- Wijnands, R., van der Klis, M. A millisecond pulsar in an X-ray binary system. *Nature* 394, 344–346, 1998.